Activation of Bacterial Ribonuclease P by Macrolides[†]

Chrisavgi Toumpeki, Anastassios Vourekas, Dimitra Kalavrizioti, Vassiliki Stamatopoulou, and Denis Drainas*

Department of Biochemistry, School of Medicine, University of Patras, 26500 Patras, Greece

Received July 26, 2007; Revised Manuscript Received January 30, 2008

ABSTRACT: The effect of macrolide antibiotic spiramycin on RNase P holoenzyme and M1 RNA from *Escherichia coli* was investigated. Ribonuclease P (RNase P) is a ribozyme that is responsible for the maturation of 5′ termini of tRNA molecules. Spiramycin revealed a dose-dependent activation on pre-tRNA cleavage by *E. coli* RNase P holoenzyme and M1 RNA. The K_s and V_{max}, as well as the $K_{s(app)}$ and $V_{max(app)}$ values of RNase P holoenzyme and M1 RNA in the presence or absence of spiramycin, were calculated from primary and secondary kinetic plots. It was found that the activity status of RNase P holoenzyme and M1 RNA is improved by the presence of spiramycin 18- and 12-fold, respectively. Primer extension analysis revealed that spiramycin induces a conformational change of the P10/11 structural element of M1 RNA, which is involved in substrate recognition.

The capability of RNA and especially catalytic RNA to act as a specific sensor of large or small molecules is central to its diverse biological functions. In addition, its ability to interact through sequence- or structure-specific hybridization with other nucleic acids gave the opportunity to the researchers worldwide to use catalytic RNA molecules as tools with enhanced catalytic properties as well as molecular targets for specific inactivation (*1*).

The search for small-molecule effectors as selective RNA ligands was driven by early observations that certain antibiotics could inhibit protein synthesis through interactions with the ribosome. The ribosome, a synthesis machine of a 2.5 MDa ribonucleoprotein assembly, is the largest ribozyme in nature characterized thus far (*2*). Confirming earlier biochemical work, the detailed structural data of ribosome−antibiotic complexes have revealed that the natural products interact predominantly with the RNA components of the ribosome and provide a useful tool for the design of specific inhibitors, even for each pathogen individually (*2*).

One of the few ribozymes of ancestral origin still represented in contemporary cells is ribonuclease P (RNase P). RNase P catalyzes a specific endonucleolytic cleavage, which removes the 5′ leader sequence from all precursor tRNA molecules, except for the primary transcript of the opal suppressor phosphoserine tRNA gene from human and *Xenopus* that it does not contain a 5′ leader sequence (*3*). It is a ribonucleoprotein in mostly all forms studied, consisting of a single RNA component and one (bacteria) or more (Archaea and eukaryotes) protein subunits (*4–6*). The RNA component from bacteria, one of the first catalytic RNA molecules identified, is responsible for the main catalytic function of the RNase P holoenzyme (*7*) and is a well-studied target, along with the holoenzyme, for various effector molecules (*8*).

Much of the early work on small molecule effectors on ribozymes was focused specifically on aminoglycosides. Today, it is known that, as well as being among the compounds that bind to the 16S rRNA, aminoglycosides also act as inhibitors of nearly all known naturally occurring ribozymes, including both bacterial and eukaryotic RNase P enzymes, through binding to their essential RNA subunit. Apart from aminoglycosides, there are several other small ligands, such as puromycin, amicetin, blasticidin S, porphyrins, porphynes, retinoids, arotinoids, calcipotriol, and anthralin, that modulate RNase P activity (ref *8* and references therein).

Macrolide antibiotics are an important therapeutic class of ribosome-targeted antibiotics. They inhibit bacterial protein synthesis by binding to the 50S ribosomal subunit in domain V of the 23S rRNA and to the pocket located between the hydrophobic crevice and the tunnel constriction and causing premature dissociation of the peptide during translation (*9*). Crystallography studies of bacterial and archaeal 50S subunits provided the detailed description of their mode of action as well as the explanation of the resistance that certain rRNA mutations provide against macrolides (*10, 11*).

In the present study, we investigated the effect of several macrolides on *Escherichia coli* RNase P activity. We have found that macrolides, in contrast to their inhibitory effect on ribosome, enhance *E. coli* RNase P activity. Detailed kinetic analysis of the activation of *E. coli* RNase P (holoenzyme and M1 RNA) by spiramycin showed that spiramycin behaves as a nonessential activator, significantly improving the activity status of RNase P holoenzyme and M1 RNA. We also determined that spiramycin induces at least one local conformational change of the P10/11 structural element, which is related with substrate recognition.

[†] This work was supported in part by the Research Committee of Patras University, program "K. Karatheodoris".

* To whom correspondence should be addressed: Department of Biochemistry, School of Medicine, University of Patras, 26500 Patras, Greece. Telephone: +30-61-997746. Fax: +30-61-997690. E-mail: drainas@med.upatras.gr.

10.1021/bi701488q CCC: $40.75
Published on Web 03/11/2008

EXPERIMENTAL PROCEDURES

Preparation of Enzymes and Substrates. The RNase P RNA from *E. coli* (M1 RNA)[1] was generated by runoff transcription of the linearized plasmid using T7 RNA polymerase. The plasmid pDW98 containing the gene of the M1 RNA under control of the T7 promoter was linearized with BsaA1. The whole procedure was performed under standard protocols (*12*). The holoenzyme was reconstituted from M1 RNA and *E. coli* RNase P protein (C5 protein). C5 protein was purified subsequent to its overexpression for 2 h in *E. coli* cells (strain XL1-blue). The cells were transformed with the plasmid pQE30 that contains the gene of C5 protein, including a series of six histidines at the amino terminus of the protein. C5 protein purification was realized using affinity chromatography with a Ni^{2+}−nitrilotriacetic acid column, as previously described (*13*). Sodium dodecyl sulfate−polyacrylamide gel electrophoresis (SDS−PAGE), Coomasie Blue staining, and silver staining of the purified, recombinant protein revealed a single band of the expected size. Reconstituted holoenzyme resulted by mixing M1 RNA (5 nM) and C5 protein (25 nM) at a molar ratio of 1:5, respectively, in the reaction buffer [50 mM Tris/HCl at pH 7.6, 10 mM $MgCl_2$, 100 mM NH_4Cl, and 0.06 mM ethylenediaminetetraacetic acid (EDTA)] with 50% glycerol. The substrate pre-$tRNA^{Tyr}$ was generated by runoff transcription of the linearized plasmid using T7 RNA polymerase, according to standard procedures. The pre-$tRNA^{Tyr}$ was internally labeled with [α-^{32}P]GTP or in some cases [α-^{32}P]ATP.

Assay for RNase P Activity. All enzyme assays were carried out at 37 °C in the appropriate reaction buffer. For the M1 RNA, the reaction buffer contained 50 mM Tris/HCl at pH 7.6, 50 mM $MgCl_2$, and 100 mM NH_4Cl. M1 RNA needs a 30 min preincubation step at 37 °C, probably to adopt the proper folding for catalysis (refolding step). The addition of the macrolide prior or after the refolding step does not alter the level of the activation effect. The reaction mixture for the holoenzyme contained 50 mM Tris/HCl at pH 7.6, 10 mM $MgCl_2$, 100 mM NH_4Cl, and 0.06 mM EDTA. The macrolide antibiotics were preincubated with the holoenzyme for 10 min prior to the addition of the substrate.

Enzyme assays for single-turnover kinetics were carried out at 37 °C in a reaction buffer containing 50 mM 2-(*N*-morpholino)ethanesulfonic acid (MES) at pH 6, 100 mM NH_4Cl, and 50 mM $MgCl_2$ for the M1 RNA or 10 mM $MgCl_2$ and 0.06 mM EDTA for the holoenzyme in the presence of 4 nM of pre-$tRNA^{Tyr}$ and 10–40 nM of M1 RNA and the appropriate amount of C5 protein for the case of the holoenzyme reaction. The k_{obs} values at each enzyme concentration were calculated by using the equation $P_t = P_o + P_\infty(1 - e^{-k_{obs}t})$. One-way analysis of variance (ANOVA) was used to estimate the data variability. The *F* Scheffé test was used to determine which means were significantly different from each other.

The reaction products were separated on a 10% (wt/vol) denaturing polyacrylamide gel and visualized with phosphoimager Fujifilm FLA 3000. Gel bands were quantified using AIDA software. For each kinetic curve, at least three independent experiments were performed, with the standard error of the values of experimental points ranging from 6 to 15%.

Mobility Shift Assay. A ^{32}P-labeled transcript of precursor tRNA (pre-$tRNA^{Tyr}$) (1.5 nM) was incubated with various concentrations of M1 RNA (30 nM–1 μM), preincubated in the presence or absence of 1 mM spiramycin at 37 °C for 30 min, in binding buffer (50 mM Tris-acetate at pH 7, 25 mM $Ca(OAc)_2$, 100 mM NH_4OAc, and 5% glycerol) at 37 °C for 1 h. M1 RNA−substrate complexes were electrophoretically analyzed on native 6% ploy acrylamide gel in TBEM buffer (35 mM Tris, 17.5 mM boric acid, 0.1 mM EDTA, and 1 mM $MgCl_2$). After electrophoresis, gels were dried and visualized by autoradiography.

Chemical Modification of M1 RNA. In vitro transcribed M1 RNA was denatured at 74 °C for 5 min followed by slow cooling to room temperature in the presence of 1× M buffer [70 mM *N*-2-hydroxyethylpiperazine-*N*′-2-ethanesulfonic acid (HEPES) at pH 7.8, 270 mM KOAc, and 10 mM MgOAc]. A total of 2 μg of M1 RNA was then mixed with spiramycin (100 or 500 μM) at 37 °C for 1 h. After the addition of 1 mM dithiothreitol (DTT), the RNAs were modified by dimethyl sulfide (DMS) (1:1000) or carbodiimidemetho-*p*-toluenesulfonate (CMCT) (21 mg/mL) at 30 °C for 8 and 30 min, respectively. Reactions were stopped with the addition of 0.2 M β-mercaptoethanol and 0.3 M NaOAc at pH 6, respectively. Modified RNAs were precipitated with ethanol and resuspended in 10 mM Tris-acetate at pH 7.9 at a final concentration of 1 pmol/μL.

Primer Extension of M1 RNA. The oligos A (5′-AGGTGAAACTGACCGATAAGC-3′ hybridizing at nucleotides 377–357) and B (5′-GGGTGGACTTTACCGTGC-3′ hybridizing at nucleotides 242–225) were used. A total of 5 pmol of each primer were 5′-labeled with ^{32}P by 10 units of T4 polynucleotide kinase (Takara) in the presence of 30 μCi γ-[^{32}P]ATP at 37 °C for 1 h. The labeled oligos were purified using Mini Quick Spin oligo columns (Roche). Approximately 2 pmol of unmodified and modified M1 RNA were mixed with 0.1 pmol of 5′-labeled primer in hybridization buffer (1.25 M KOAc, 1 mM EDTA, and 10 mM Tris-acetate at pH 7.9) heated at 80 °C for 10 min and then cooled slowly to 47 °C. The RNA was reverse-transcribed in the presence of 5 units of AMV RT (Finnzymes), 5 mM MgOAc, 2.5 mM DTT, and 0.5 mM dNTPs at 47 °C for 45 min. For sequencing reactions, ddNTPs were present at a final concentration of 0.18 mM. The reaction mixtures were phenol-extracted, and the cDNA products were precipitated by ethanol, analyzed by denaturing 6% PAGE, and visualized by autoradiography.

RESULTS

Kinetic Analysis. The macrolides, spiramycin (Figure 1A), erythromycin, tylosin, and roxithromycin, revealed a dose-dependent activating effect on *E. coli* RNase P holoenzyme and M1 RNA, with spiramycin being the most potent activator. The activating effect reaches a maximum value at a low micromolar range, whereas, at concentrations up to 1 mM, macrolides showed no effect on *Dictyostelium discoideum* RNase P activity (data not shown). The substrate for RNase P assays was *in vitro* labeled of the *E. coli* precursor $tRNA^{Tyr}$ gene. Figure 1B shows the dose-dependent activat-

[1] Abbreviations: M1 RNA, *E. coli* RNase P RNA; C5 protein, *E. coli* RNase P protein; SDS−PAGE, sodium dodecyl sulfate−polyacrylamide gel electrophoresis; EDTA, ethylenediaminetetraacetic acid.

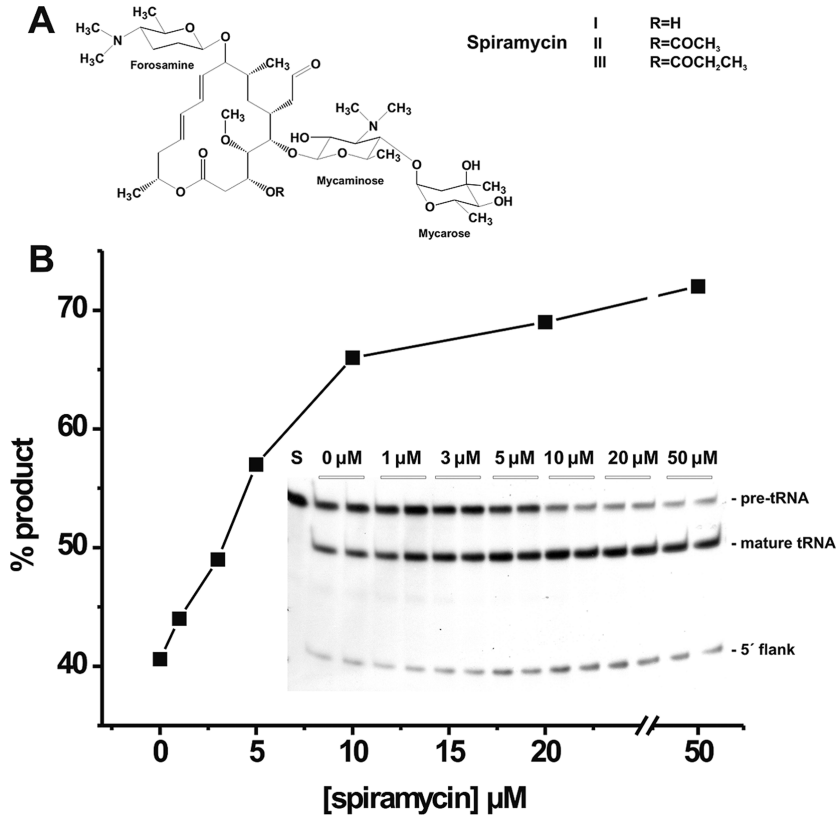

FIGURE 1: (A) Chemical structure of spiramycin (pK = 7.9). (B) Dose-dependent activation of *E. coli* RNase P by spiramycin. Enzyme assays were performed in the absence or presence of spiramycin (CAS number 8025-81-8) at the concentrations indicated (inset). Lane S: substrate alone. In the right-hand margin, the bands corresponding to the precursor and mature tRNA molecules as well as the 5′ leader sequence are indicated.

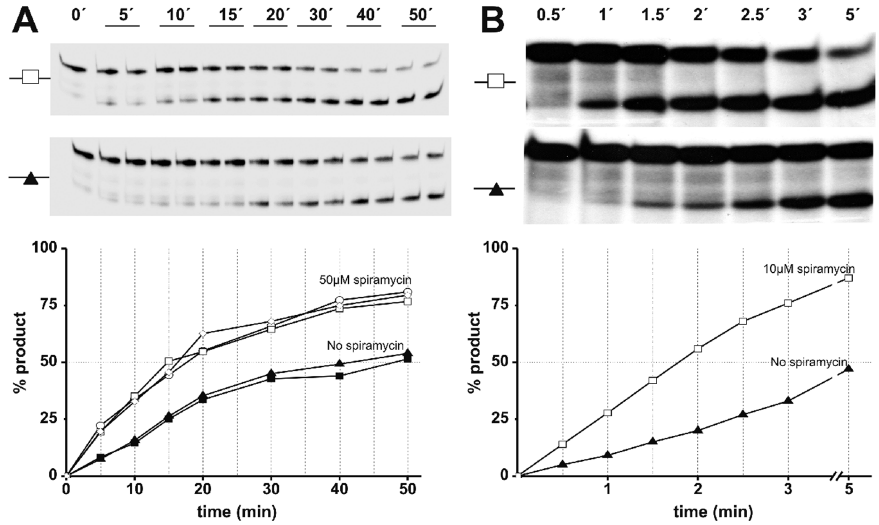

FIGURE 2: Time plot of the M1 RNA (A) and RNase P holoenzyme (B) reaction, in the absence or presence of spiramycin. (A) Effect of various preincubation steps on the M1 RNA reaction in the absence (■ and ▲) or in the presence (□, ○, and ◇) of 50 μM spiramycin. (■) 30 min of preincubation (refolding step), (▲) 60 min of preincubation, (□) 30 min of refolding followed by 30 min of preincubation in the presence of spiramycin, (○) 30 min of refolding and no preincubation with spiramycin, and (◇) 30 min of refolding in the presence of spiramycin. A representative autoradiography for each group of curves is provided atop the graph. Reactions are in duplicate for each time point. (B) Time plot of the holoenzyme reaction in the absence (▲) and presence (□) of 10 μM spiramycin.

ing effect of spiramycin on *E. coli* RNase P holoenzyme. Preincubation of holoenzyme with spiramycin (not shown) or preincubation of the refolded M1 RNA in the absence or presence of spiramycin prior to the addition of the substrate did not alter the activating effect of the antibiotic on RNase P activity (Figure 2A). The initial velocity in the presence or absence of spiramycin was determined from the initial slopes of time plots (Figure 2B). To examine the type of activation of spiramycin on RNase P activity, double-reciprocal plots (1/v versus 1/[S]) were obtained. Figure 3 shows double-reciprocal plots with increasing concentrations of spiramycin. As can be seen from these plots, the apparent V_{max} value (intercept of the 1/v axis) increases from 0.42 (control) to 0.68 pmol min^{-1} (50 μM spiramycin), while the

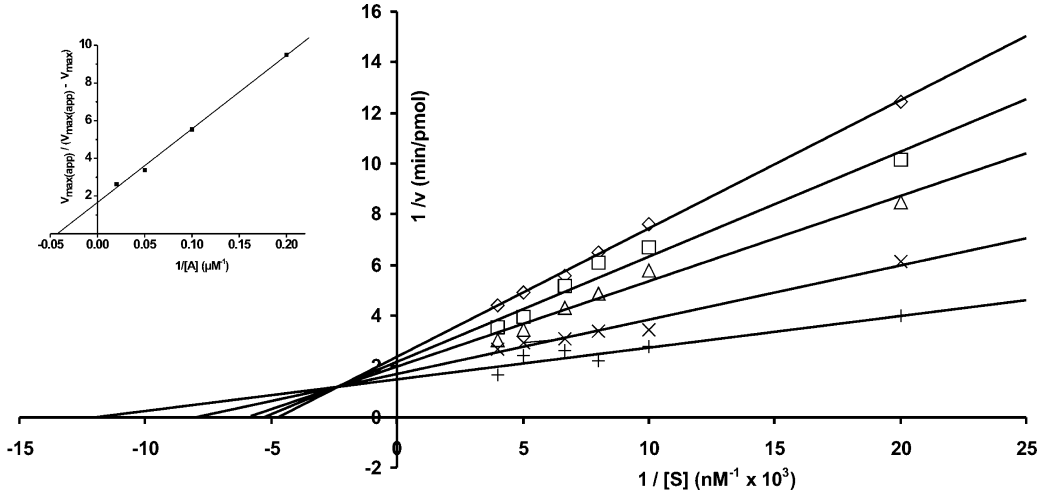

FIGURE 3: Double-reciprocal plot ($1/v$ versus 1/[pre-tRNA]) for the RNase P reaction in the presence of various concentrations of spiramycin. (◇) 0 μM of spiramycin (control), (□) 5 μM of spiramycin, (△) 10 μM of spiramycin, (×) 20 μM of spiramycin, and (+) 50 μM of spiramycin. (Inset) Variation of $V_{max(app)}/(V_{max(app)} - V_{max})$ as a function of 1/[A] (eq 3). The linearity of this plot indicates that one molecule of spiramycin participates noncooperatively in the kinetic mechanism of activation. The V_{max} and $V_{max(app)}$ are calculated from the corresponding double-reciplocal plots.

apparent K_S decreases from 213 to 106 nM. It is clear from these results that the activation is of a mixed type and spiramycin is a nonessential activator (*14*). A simple model that can explain these results is the following:

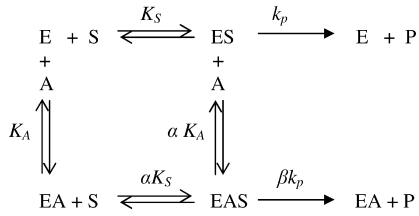

where E is RNase P, S is pre-tRNA, A is the activator (spiramycin), P is tRNA, K_S is the dissociation constant of the ES complex, αK_S is the dissociation constant of the EAS complex (equation EA + S → EAS), K_A is the dissociation constant of the EA complex, αK_A is the dissociation constant of the EAS complex (equation ES + A → EAS), k_p is the rate constant for the breakdown of ES to E and P, and βk_p is the rate constant for the breakdown of EAS to EA and P. The differential rate law, corresponding to the above kinetic scheme involving one activation site is given by the equation

$$v = \frac{V_{max}\frac{[S]}{K_S} + \beta V_{max}\frac{[A][S]}{\alpha K_A K_S}}{1 + \frac{[S]}{K_S} + \frac{[A]}{K_A} + \frac{[A][S]}{\alpha K_A K_S}} \quad (1)$$

Therefore, the apparent maximum velocity is given by the equation

$$V_{max(app)} = \frac{V_{max}\left(1 + \frac{\beta[A]}{\alpha K_A}\right)}{\left(1 + \frac{[A]}{\alpha K_A}\right)} \quad (2)$$

Further information for the type of activation can be taken from secondary kinetic plots. The slope replot (inset in Figure 4) and intercept replot (not shown) taken from double-reciprocal plots of Figure 3 are hyperbolic. In contrast to mixed-type inhibition, these replots are descending curves,

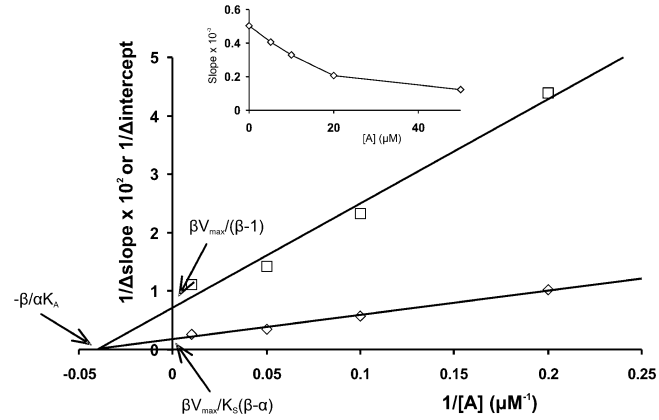

FIGURE 4: Secondary replot of 1/Δ slope and 1/Δ intercept versus 1/[A]. The Δ slope and Δ intercept were taken as a control value minus the "plus activator" value from the slopes and the $1/v$ axis intercepts of the double-reciprocal plots (Figure 3). The intercept of the 1/Δ slope axis is equal to $\beta V_{max}/K_S(\beta - \alpha)$, and the intercept of the 1/Δ intercept axis is equal to $\beta V_{max}/(\beta - 1)$. The 1/[A] axis gives $-\beta/\alpha K_A$. The values of the factors α and β are 0.14 and 2.52, respectively. (Inset) Slope replot of double-reciprocal plots (Figure 3) versus [A]. The slope is hyperbolic, characteristic of mixed-type nonessential activation.

characteristic for mixed-type nonessential activation. From the secondary reciprocal plots of 1/Δ slope and 1/Δ intercept versus 1/[A] (Figure 4), βV_{max} ($V_{max(app)}$), αK_S ($K_{S(app)}$), and K_A values of the above model can be calculated. The respective values are $V_{max(app)} = 1.06$ pmol min^{-1}, $K_{S(app)} = 30$ nM, and $K_A = 450$ nM. The values of the factors α and β are 0.14 and 2.52, respectively. At a saturating concentration of spiramycin, the apparent V_{max} value for the holoenzyme (reconstituted RNase P) increases 2.5-fold and the apparent K_S value decreases 7.1-fold. The concentration of the holoenzyme is considered to be equal to the concentration of M1 RNA (5 nM). Therefore, if we consider that all of the amount of M1 RNA used in the reaction has the proper conformation for activity then the catalytic rate constants, k_{cat} and $k_{cat(app)}$ of the holoenzyme, in the absence or presence of spiramycin, are calculated to be 4.22 and 10.6 min^{-1}, respectively. The same kinetic examination was carried out for M1 RNA (not shown). The apparent V_{max} value increases

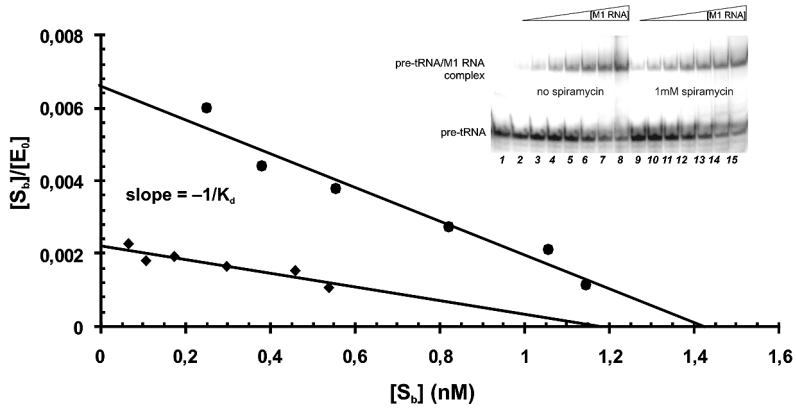

FIGURE 5: Scatchard plot for binding of pre-tRNA^{Tyr} substrate to M1 RNA, where [S_b] is [substrate bound] and [E_0] is [total enzyme]. Complexes where formed between a constant amount of substrate (1.5 nM) and M1 RNA from 30 nM to 1 μM, in the absence (◆) and presence (●) of 1 mM spiramycin. appK_d values were determined from the reciprocal of the slopes of the lines. (Inset) Autoradiography of a representative gel shift assay of the binding of pre-tRNA^{Tyr} substrate to M1 RNA. Lane 1, substrate alone; lanes 2–8, substrate and M1 RNA incubated in the absence of spiramycin; lanes 9–15, substrate and M1 RNA incubated in the presence of 1 mM spiramycin.

from 0.19 (control) to 0.39 (50 μM spiramycin) pmol min^{-1}, while the apparent K_S decreases from 518 to 232 nM. The corresponding βV_{max} ($V_{max(app)}$), αK_S ($K_{S(app)}$), and K_A values are 0.456 pmol min^{-1}, 104 nM, and 80 nM, respectively. The values of the factors α and β for the M1 RNA activation are 0.2 and 2.4, respectively. Also, the catalytic rate constants, k_{cat} and $k_{cat(app)}$ of the M1 RNA, in the absence or presence of spiramycin, are calculated to be 1.9 and 4.56 min^{-1}, respectively. At a saturating concentration of spiramycin, the apparent V_{max} value for the M1 RNA increases 2.4-fold and the apparent K_S value decreases 5-fold. The estimation of the spiramycin interaction coefficient with RNase P holoenzyme or M1 RNA was based on the relationship between $V_{max(app)}/(V_{max(app)} - V_{max})$ and the reciprocal of the spiramycin concentration. From eq 2, it follows that

$$\frac{V_{max(app)}}{V_{max(app)} - V_{max}} = \frac{\beta}{\beta - 1} + \frac{1}{[A]}\frac{aK_A}{(\beta - 1)} \qquad (3)$$

From this equation, it is obvious that the plot $V_{max(app)}/(V_{max(app)} - V_{max})$ versus 1/[A] is linear only when one molecule of spiramycin participates noncooperatively in the kinetic mechanism of activation. Indeed, this seems to be the case (inset in Figure 3). Equation 3 is valid when the interaction coefficient is equal to 1. If n molecules of spiramycin interact with the enzyme, eq 3 becomes

$$\frac{V_{max(app)}}{V_{max(app)} - V_{max}} = \frac{\beta}{\beta - 1} + \frac{1}{[A]^n}\frac{aK_A}{(\beta - 1)} \qquad (4)$$

Determination of the appK_d. To determine the appK_d values for the substrate in the presence and absence of spiramycin, we conducted electophoretic mobility shift assays in 6% native polyacrylimide gels (see the Experimental Procedures). To prevent substrate hydrolysis, the binding assays were performed in the presence of 25 mM Ca^{2+} (*15*). The corresponding appK_d values in the absence (appK_d = 526 nM) or presence (appK_d = 222 nM) of spiramycin were calculated from the slopes of the Scatchard plots (Figure 5).

Footprinting Analysis. In an attempt to identify the binding sites of spiramycin on the M1 RNA, we conducted footprinting analysis. M1 RNA was modified with DMS, CMCT, and kethoxal in the presence and in the absence of 100 and 500 μM spiramycin. Primer extension analysis modified with DMS M1 RNA in the presence of spiramycin revealed two sites (A124 and A129) where the premature termination was increased (Figure 6). It seems that the conformational changes, induced in the presence of spiramycin, expose A124 and A129 to DMS modification. CMCT modification failed to provide possible binding sites of spiramycin, while the results from the use of kethoxal were inconclusive.

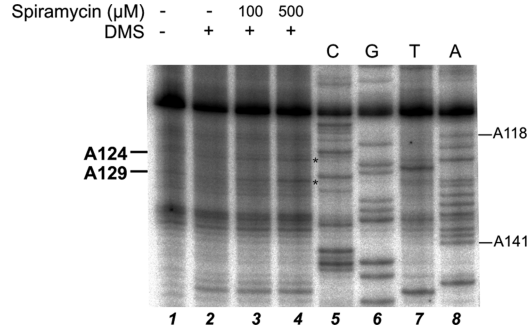

FIGURE 6: Primer extension analysis and dideoxy sequencing of M1 RNA. Unmodified (lane 1) and DMS-treated M1 RNA (lanes 2−4) were extended with reverse transcriptase using oligo B. The sequencing ladder reactions were generated by extending the *in vitro* transcript of the RNase P RNA gene in the presence of ddNTPs (lanes C-, G-, T-, and A-coding strand). Bands representing new premature ending sites appearing when spiramycin is bound on the RNA prior to modification (lanes 3 and 4) are noted on the left margin (A124 and A129, also marked with asterisks), while position markers are on the right.

DISCUSSION

The detailed kinetic analysis of the activation of *E. coli* RNase P activity by spiramycin presented in this paper showed that spiramycin acts as a mixed-type nonessential activator. At a saturating concentration of spiramycin, the apparent V_{max} value for the holoenzyme (reconstituted RNase P) increases 2.5-fold and the apparent K_S value decreases 7.1-fold, while for the M1 RNA reaction, the same values increase 2.4- and decrease 5-fold, respectively. It is obvious that spiramycin considerably improves the catalytic coefficient and the affinity for the substrate of the RNase P holoenzyme and M1 RNA. From the estimation of the spiramycin interaction coefficient with RNase P holoenzyme

or M1 RNA, it was deduced that one molecule of spiramycin participates noncooperatively in the kinetic mechanism of activation. Because of the fact that the stoichiometry was deduced by a kinetic curve rather than from a real measurement of the amount of bound spiramycin, we can not exclude the existence of additional spiramycin-binding sites on RNase P that do not kinetically participate in the proposed model.

A better picture for the evaluation of the activity status of RNase P holoenzyme or M1 can be taken from the calculation of the k_{cat}/K_S ratio. Therefore, in the absence of spiramycin, k_{cat}/K_S (calculated from the primary kinetic plots) is equal to 3.3×10^5 s^{-1} M^{-1} for the holoenzyme and 6.1×10^4 s^{-1} M^{-1} for M1 RNA. At a saturating concentration of the activator, the $k_{cat(app)}/K_{S(app)}$ ratio (calculated from secondary kinetic plots) is equal to 5.9×10^6 s^{-1} M^{-1} for the holoenzyme and 7.3×10^5 s^{-1} M^{-1} for M1 RNA. These findings suggest that spiramycin improves the activity status of RNase P holoenzyme (18-fold) and M1 RNA (12-fold) significantly. These results also indicate that the presence of protein does not prevent macrolides to induce the proper conformational changes to RNase P RNA needed for maximum activation. In addition, the observed k_{cat}/K_S values ($<10^7$ s^{-1} M^{-1}) reveal that the formation of the encounter complex between the substrate and enzyme is rapidly equilibrated ($K_M = K_S$) (*16*). It is interesting to note that, as should be expected, the K_S values, estimated by the kinetic examination for M1 RNA, and the appK_d values, estimated by electophoretic mobility shift assays, in the presence and absence of spiramycin, are almost identical.

To examine whether the spiramycin affects the catalytic step of the reaction, single-turnover kinetics were performed at pH 6, where the chemical step is rate-limiting (data not shown). It was revealed that the presence of spiramycin increases the catalytic rate constant (k_{obs}) of the holoenzyme and M1 RNA. More specifically, at 50 μM spiramycin, the k_{obs} increases from 1.06 to 1.25 min^{-1} (F Scheffé test, $p < 0.05$) for the holoenzyme and from 0.8 to 1.29 min^{-1} (F Scheffé test, $p < 0.001$) for the M1 RNA. At this concentration of spiramycin, the k_{obs} value for the holoenzyme and M1 RNA increases 1.18- and 1.6-fold, respectively. It is obvious that the presence of spiramycin affects the catalytic step of the reaction.

In an attempt to investigate the nature of the interaction between the ribozyme and spiramycin (pK = 7.9), we screened the pH from 5 to 9 in the presence and absence of the effector molecule. It was revealed that the activation effect of spiramycin remained at the same level regardless of the pH changes (not shown). This implies that hydrophobic interactions might play an important role in promoting macrolide binding to the ribozymes, as it was reported for the ribosome (*17*). In addition, no change to the activation effect (supression or enhancement) of the macrolide was observed when [Mg^{2+}] was screened from 10 to 100 mM for the holoenzyme and M1 RNA (not shown). It can be speculated that magnesium and spriramycin do not have overlaping binding sites and that magnesium does not mediate in the binding of spiramycin to the enzyme.

Moreover, as evidenced by primer extension analysis, binding of spiramycin results in increased DMS modification of residues A124 and A129, with the latter being more prominent. This indicates a structural rearrangement of the P10/11 region, which harbors residues involved in substrate interaction (*18, 19*). Residue A124 (*E. coli* numbering) is a conserved residue in bacterial RNase P RNAs, a fact that underscores its functional importance, as well as the significance of the observed phenomenon. CMCT modification failed to provide additional data, while the results from the use of kethoxal were inconclusive. It is reasonable to assume that this new conformation induced by the binding of spiramycin has increased affinity for the substrate of the enzyme and/or releases the reaction products more readily as evidenced by our kinetic analysis. It is important to note that the fact that the activity of *D. discoideum* RNase P is not affected by spiramycin could be due to a different architecture of the P10/11 element (*20*). Considering the aforementioned results, we conclude that the macrolide mode of action is distinct compared to the activation of RNase P ribozyme by its protein component. More specifically, it does not lower the Mg^{2+} dependence, and it induces a local change in the conformation of the P10/11 element, rather than a wider stabilization effect as the protein subunit does. However, the activation effect is most probably mediated by improving substrate-binding and positioning in the enzyme's active site.

Antibiotics, similar to other secondary metabolites, should be seen as effector molecules in the regulation of many biological activities and surely not only as inhibitors but rather as modulators. A very good example supporting this notion was known for many years (since 1965). Streptomycin-dependent ribosomes that show altered translation accuracy leading to hyperaccurate ribosomes can confer bacterial resistance and sometimes dependence on streptomycin for the cellular survival (*21*). From this point of view, the antibiotic is a positive effector molecule, because it is absolutely required for viability. In agreement to this observation, it has been reported that the aminoglycoside antibiotic neomycin B instead of inhibiting can actually promote the cleavage reaction that is catalyzed by the hairpin ribozyme, by providing the appropriate positively charged environment for the ribozyme to obtain its catalytically active folding (*22*). Also, in a recent study, it was shown that aminoclycosides promote self-splicing of the *Cr.psbA2* group I intron at subthreshold Mg^{2+} concentrations, with neomycin being the most effective of the aminoglycosides tested (*23*). Furthermore, the antibiotic viomycin enhances the self-cleavage of the *Neurospora crassa* VS ribozyme and, at the same time, decreases the amount of magnesium that is required for activity. It also stimulates the trans-cleavage reaction by facilitating the interaction between negatively charged RNA molecules (*24*). In addition, in a study where the large ribosomal subunit from *Thermus aquaticus* was reconstituted *in vitro* in the absence of 5S rRNA, it was shown that the omission of 5S rRNA can be partly compensated by the presence of some ribosome-targeted antibiotics of the macrolide, ketolide, or streptogramin B groups (*25*).

The application of *E. coli* RNase P RNA in gene inactivation was achieved by attaching covalently a guide sequence (GS), complementary to a RNA target, to the 3′ end of M1 RNA (M1GS) (*26*). This modification converts the M1GS from a structure-specific ribozyme to a sequence-specific one. The concept of this modification is that when the GS binds to the target RNA a structure equivalent to the top portion of a precursor tRNA (the minimal requirement

for substrate recognition of M1 RNA) can be formed. Then, the M1GS RNA hydrolyzes successfully the target RNA. Thus, the effect of macrolides on M1 RNA shows that this certain class of antibiotics could have a dual role in therapy. Apart from their role in the battle against pathogens, the M1GS RNA−macrolide complex, taking into account the fact that macrolides do not have any effect on eukaryotic RNase P, could become a valuable tool in gene inactivation.

Macrolides can become useful tools for the dissecting of the catalytic properties of RNase P ribozymes, whether they might be naturally occurring or engineered for therapeutical purposes. The elucidation of their mode of action can provide clues for the use of specific chemical and/or mutational modifications on RNase P ribozymes for the improvement of their catalytic potential. Such studies could give some new perspective to gene inactivation through ribozyme techniques, which is lately overridden by siRNA applications.

ACKNOWLEDGMENT

We thank Professor Sidney Altman for discussion and critical reading of the manuscript. We thank Dr. Dimitrios Kalpaxis and Dr. George Dinos for discussion and Dr. Constantinos Stathopoulos for critical reading of the manuscript. The plasmids pDW98/M1RNA and pQE30/C5 were generous gifts of Professor Roland Hartmann.

REFERENCES

1. Schroeder, R., Waldsich, C., and Wank, H. (2000) Modulation of RNA function by aminoglycoside antibiotics. *EMBO J. 19*, 1–9.
2. Steitz, T. A., and Moore, P. B. (2003) RNA, the first macromolecular catalyst: The ribosome is a ribozymes. *Trends Biochem. Sci. 28*, 411–418.
3. Lee, B. J., De La Pena, P., Tobian, J. A., Zasloff, M., and Hatfield, D. (1987) Unique pathway of expression of an opal suppressor phosphoserine tRNA. *Proc.Natl. Acad. Sci. U.S.A. 84*, 6384–6388.
4. Frank, D. N., and Pace, N. R. (1998) Ribonuclease P: Unity and diversity in a tRNA processing ribozymes. *Annu. Rev. Biochem. 67*, 153–180.
5. Pannucci, J. A., Haas, E. S., Hall, T. A., Harris, J. K., and Brown, J. W. (1999) RNase P RNAs from some Archaea are catalytically active. *Proc. Natl Acad. Sci. U.S.A. 96*, 7803–7808.
6. Xiao, S., Scott, F., Fierke, C. A., and Engelke, D. R. (2002) Eukaryotic ribonuclease P: A plurality of ribonucleoprotein enzymes. *Annu. Rev. Biochem. 71*, 165–189.
7. Guerrier-Takada, C., Gardiner, K., Marsh, T., Pace, N., and Altman, S. (1983) The RNA moiety of ribonuclease P is the catalytic subunit of the enzyme. *Cell 35*, 849–857.
8. Vourekas, A., Kalavrizioti, D., Stathopoulos, C., and Drainas, D. (2006) Modulation of catalytic RNA biological activity by small molecule effectors. *Mini Rev. Med. Chem. 6*, 971–978.
9. Hermann, T. (2005) Drugs targeting the ribosome. *Curr. Opin. Struct. Biol. 15*, 355–366.
10. Pfister, P., Jenni, S., Poehlsgaard, J., Thomas, A., Douthwaite, B. N., and Bottger, E. C. (2004) The structural basis of macrolide−ribosome binding assessed using mutagenesis of 23S rRNA positions 2058 and 2059. *J. Mol. Biol. 342*, 1569–1581.
11. Weisblum, B. (1995) Insights into erythromycin action from studies of its activity as inducer of resistance. *Antimicrob. Agents Chemother. 39*, 597–805.
12. Milligan, J. F., Groebe, D. R., Witherell, G. W., and Uhlenbeck, O. C. (1987) Oligoribonucleotide synthesis using T7 RNA polymerase and synthetic DNA templates. *Nucleic Acids Res. 15*, 8783–8798.
13. Rivera-Leon, R., Green, C. J., and Vold, B. S. (1995) High-level expression of soluble recombinant RNase P protein from *Escherichia coli*. *J. Bacteriol. 177*, 2564–2566.
14. Segel, I. H. (1975) *Enzyme Kinetics*, Wiley-Interscience, New York.
15. Buck, A. H., Dalby, A. B., Poole, A. W., Kazantsev, A. V., and Pace, N. R. (2005) Protein activation of a ribozyme: The role of bacterial RNase P protein. *EMBO J. 24*, 3360–3368.
16. Fersht, A. (1999) *Structure and Mechanism in Protein Science: A Guide to Enzyme Catalysis and Protein Folding*, W. H. Freeman and Company, New York.
17. Christian, E. L., Zahler, N. H., Kaye, N. M., and Harris, M. E. (2002) Analysis of substrate recognition by the ribonucleoprotein endonuclease RNase P. *Methods 28*, 307–322.
18. LaGrandeur, T. E., Hüttenhofer, A., Noller, H. F., and Pace, N. R. (1994) Phylogenetic comparative chemical footprint analysis of the interaction between ribonuclease P RNA and tRNA. *EMBO J. 13*, 3945–3952.
19. Hansen, J. L., Ippolito, J. A., Ban, N., Nissen, P., Moore, P. B., and Steitz, T. A. (2002) The structure of four macrolide antibiotics bound to the large ribosomal subunit. *Mol. Cell 10*, 117–128.
20. Marquez, S. M., Harris, J. K., Kelley, S. T., Brown, J. W., Dawson, S. C., Roberts, E. C., and Pace, N. R. (2005) Structural implications of novel diversity in eucaryal RNase P RNA. *RNA 11*, 739–751.
21. Davies, J., Gorini, L., and Davis, B. D. (1965) Misreading of RNA codewords induced by aminoglycoside antibiotics. *Mol. Pharmacol. 1*, 93–106.
22. Earnshaw, D. J., and Gait, M. J. (1998) Hairpin ribozyme cleavage catalyzed by aminoglycoside antibiotics and the polyamine spermine in the absence of metal ions. *Nucleic Acid Res. 26*, 5551–5561.
23. Bao, Y., and Herrin, D. L. (2006) Mg^{2+} mimicry in the promotion of group I ribozyme activities by aminoglycoside antibiotics. *Biochem. Biophys. Res. Commun. 344*, 1246–1252.
24. Olive, J. E., De Abreu, D. M., Rastogi, T., Andersen, A. A., Mittermaier, A. K., Beattie, T. L., and Collins, R. A. (1995) Enhancement of *Neurospora* VS ribozyme cleavage by tuberactinomycin antibiotics. *EMBO J. 14*, 3247–3251.
25. Khaitovich, P., and Mankin, S. (1999) Effect of antibiotics on large ribosomal subunit assembly reveals possible function of 5 S rRNA. *J. Mol. Biol. 291*, 1025–1034.
26. Gopalan, V., Vioque, A., and Altman, S. (2002) RNase P: Variations and uses. *J. Biol. Chem. 277*, 6759–6762.

BI701488Q